Accurate Analytical Single-Photoelectron Response of Silicon Photomultipliers

Davide Marano, Massimiliano Belluso, Giovanni Bonanno, Sergio Billotta, Alessandro Grillo, Salvatore Garozzo, and Giuseppe Romeo

***Abstract*— This paper addresses a comprehensive analytical analysis of a new accurate electrical model of silicon photomultiplier (SiPM) detectors. The adopted circuit model allows to truly reproduce the SiPM output signal waveform apart from the specific technology employed for the fabrication process, and can also be profitably exploited to perform reliable circuit-level simulations. A novel analytical expression of the transient single-photoelectron response due to photon absorption is systematically developed. The attained function accurately reproduces the fast detector ignition, ensuing avalanche self-quenching, and final slow recharging operation. Predictive capabilities of the adopted analytical model are demonstrated by means of experimental measurements on a real detector.**

***Index Terms*— Analytical waveforms, electrical model, SiPM, small-signal analysis, time constants, transient response.**

I. Introduction

SILICON photomultipliers (SiPMs), also referred to as multi-pixel photon counters (MPPCs), are a favourable class of semiconductor-based photodetectors addressing the challenge of detecting, timing and quantifying low-light optical signals down to the single-photon counting level. SiPMs offer a highly attractive alternative that closely mimics the low-light detection capabilities of traditional photomultiplier tubes, while providing all the benefits of a solid-state device.

The extremely remarkable performance achieved by SiPM sensors in terms of high photon detection efficiency, fast transient response, excellent timing resolution, and wide spectral range, has made considerable research activities and technological development to be constantly devoted to SiPM devices within the scientific community involved in medical imaging, high-energy physics and astrophysics. Contextually, the electronics development aims at the realization of specifically designed front-end architectures to acquire, preserve and reproduce the SiPM output electrical signals.

Essential prerequisite for a successfully designed read-out configuration is an accurate equivalent electrical model of the SiPM detector allowing a reliable interpretation of its physical interactions with the conditioning electronics. A careful theoretical study of both static and dynamic characteristics of the silicon detector as a signal source is therefore required to help choose the most performing front-end solutions.

In this scenario, the availability of a truthful analytical expression of the SiPM response, along with the possibility of performing reliable circuit-level simulations, becomes a key point of the design phase, since the main characteristics of the achieved functions can be profitably related to the model parameters of both SiPM detectors and front-end electronics. In addition, on the basis of a complete analytical model, the core physical properties of the SiPM detectors can be functionally related to the equivalent circuit parameters regardless of the particular fabrication technology.

This work develops a detailed analytical investigation of an accurate electrical model of the SiPM detectors. Although different SiPM electrical characterizations are reported in literature, analytical research studies of the adopted models are still poor [1]–[9]. A new accurate analytical expression for the single-photoelectron response is hereby derived and discussed. Functional relationships are provided for the most crucial parameters involved in the model, and the associated curve plots are critically analyzed. SPICE simulations along with experimental measurements on a real device are finally proved to be in good agreement with the achieved analytical expressions.

The adopted analysis turns out to be particularly helpful for designing an optimum front-end architecture for SiPM detectors, since the performance of the entire detection system, especially in terms of dynamic range and timing resolution, can be accurately predicted as a function of both SiPM model parameters and coupled front-end electronics.

II. SiPM Electrical Model

SiPM detectors basically have a physical structure in which combinations of a Geiger-mode avalanche photodiode micropixel and a series quenching resistor are connected in parallel and bi-dimensionally arranged in a matrix configuration.

The equivalent model simulating the discharge of N_f active microcells for a SiPM detector consisting of a total number of N microcells is depicted in Fig. 1. The circuit is separated into an active component for the N_f fired pixels and a passive part for the remaining $N_p = N\text{-}N_f$ unfired microcells.

For each individual pixel, R_d is the internal resistance of the diode space-charge and quasi-neutral regions, C_d is the

Manuscript received November 7, 2013; revised January 10, 2014; accepted April 2, 2014. Date of publication April 9, 2014; date of current version July 1, 2014. This work was supported in part by the ASTRI Flagship Project, financed by the Italian Ministry of Education, University and Research (MIUR) and led by the Italian National Institute for Astrophysics (INAF). The associate editor coordinating the review of this paper and approving it for publication was Prof. Ralph Etienne-Cummings.

The authors are with INAF, Osservatorio Astrofisico di Catania, Catania I-95123, Italy (e-mail: dmarano@oact.inaf.it; mbelluso@oact.inaf.it; gbonanno@oact.inaf.it; sbillotta@oact.inaf.it; agrillo@oact.inaf.it; sgarozzo@oact.inaf.it; gromeo@oact.inaf.it).

Color versions of one or more of the figures in this paper are available online at http://ieeexplore.ieee.org.

Digital Object Identifier 10.1109/JSEN.2014.2316363

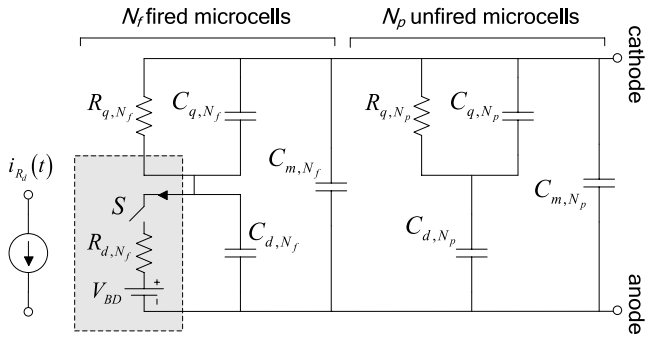

Fig. 1. SiPM equivalent electrical model. The circuit branch in the dashed box, mimicking the avalanche discharges of the firing microcells, can be opportunely replaced by a proper time-dependent current generator.

junction capacitance of the inner depletion layer, R_q and C_q are the integrated quenching resistance and parallel stray capacitance, respectively, and C_m accounts for all parasitic capacitive contributions across the two pixel terminals. A further fringe capacitance for the common cathode bonding pad should be also included in the model, but its effects can be endorsed in the parallel contribution of C_m for each single microcell.

The i-th equivalent resistances and capacitances included in the model are expressed by the following relationships

$$R_{i,N_f}=\frac{R_i}{N_f},\ \ R_{i,N_p}=\frac{R_i}{N_p},\ \ C_{i,N_f}=N_fC_i,\ \ \ C_{i,N_p}=N_pC_i. \tag{1}$$

The avalanche discharge of the firing cells can be modeled by a DC voltage supply representing the diode breakdown potential, V_{BD}, in series with a voltage-controlled switch, S. This circuit branch can be more conveniently replaced by a proper time-dependent current source representing the instantaneous current, $i_{R_d}(t)$, flowing through the equivalent diode resistance R_{d,N_f}, as sketched in the dashed box in Fig. 1.

The advantage of the latter avalanche generation model relies in the possibility of achieving a comprehensive analytical expression of the SiPM output response accurately describing all characteristic transient phases resulting from a trigger ignition (by photon absorption or thermic generation).

Based on the above considerations, the proposed analytical analysis of the SiPM output response is now discussed.

III. Small-Signal Analysis

Fig. 2 depicts the linearized small-signal equivalent circuit used for deriving the Laplace-domain analytical expression of the SiPM output current $i_{R_L}(t)$ across a resistive load R_L, representing the equivalent input resistance of the front-end electronics. The circuit directly results from the model in Fig. 1 by inverting the direction of the input source and output current and grouping capacitors C_{m,N_f} and C_{m,N_p} into the single equivalent contribution $C_{m,N}=NC_m$.

The complete small-signal transfer function of the circuit in Fig. 2 as a function of the complex frequency is found to be

$$H(s)\ =\ \frac{I_{R_L}(s)}{I_{R_d}(s)}=\frac{1+b_1's\ +b_2's^2}{1+a_1's+a_2's^2+a_3's^3}, \tag{2}$$

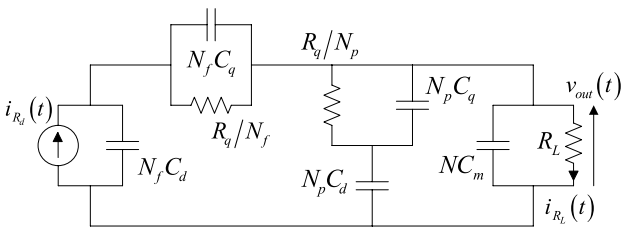

Fig. 2. SiPM small-signal equivalent model with a passive read-out circuit.

where the s-coefficients in the numerator are given by the following relationships

$$b_1'=R_q\left(C_d+2C_q\right) \tag{3}$$

$$b_2'=R_q^2C_q\left(C_d+C_q\right), \tag{4}$$

while those in the denominator are expressed by

$$a_1'=2R_q\left(C_d+C_q\right)+NR_L\left(C_d+C_m\right) \tag{5}$$

$$a_2'=R_q\Big[R_q\Big(C_d+C_q\Big)^2 +NR_L\Big(C_d^2+2C_dC_q+2C_mC_d+2C_mC_q\Big)\Big] \tag{6}$$

$$a_3'=NR_LR_q^2\left(C_d+C_q\right)\left[C_dC_q+C_m\left(C_d+C_q\right)\right]. \tag{7}$$

Collecting numerator and denominator of the transfer function in (2), an exact pole-zero cancellation occurs, leading to

$$H(s)\ =\ \frac{1+sR_q\left(C_d+C_q\right)}{1+sR_q\left(C_d+C_q\right)}\frac{1+b_1s}{1+a_1s+a_2s^2} =\ \frac{1+b_1s}{1+a_1s+a_2s^2}, \tag{8}$$

in which $b_1=R_qC_q$, while the s-coefficients of the second-order polynomial in the denominator are given by

$$a_1\ =\ R_q\left(C_d\ +C_q\right)+NR_L\left(C_d\ +C_m\right) \tag{9}$$

$$a_2\ =\ NR_LR_q\left(C_dC_q+C_dC_m+C_qC_m\right). \tag{10}$$

Since a_1^2>$4a_2$ upon any values of the passive elements, the above transfer function exhibits two real poles and can hence be more conveniently expressed as

$$H(s)\ =\ \frac{1+s\,\tau_z}{\left(1+s\tau_{p1}\right)\ \left(1+s\tau_{p2}\right)}, \tag{11}$$

in which $\tau_z\ =\ b_1$, while the associated time constants are related to the denominator s-coefficients according to

$$\tau_{p1}\ =\ \frac{a_1+\sqrt{a_1^2-4a_2}}{2} \tag{12}$$

$$\tau_{p2}\ =\ \frac{a_1-\sqrt{a_1^2-4a_2}}{2}. \tag{13}$$

As far as the input current generator is concerned, the total charge released by the avalanche events, as turns out from the physics theory of the device, is instantly collected across the equivalent resistance R_{d,N_f}, and results in a photodiode current $i_{R_d}(t)$ which abruptly jumps to its peak value, dictated by the excess bias voltage V_{OV} beyond the breakdown potential, and exponentially drops with a circuit-dependent

decay time constant. Consequently, the current $i_{R_d}(t)$ can be expressed by

$$i_{R_d}(t) = I_0 e^{-\frac{t}{\tau_d}}, \tag{14}$$

where I_0 represents the current peak value given by

$$I_0 = \frac{V_{OV}}{R_{d,N_f}} = N_f \frac{V_{OV}}{R_d} \tag{15}$$

and τ_d is the quenching time constant set by [2], [4]

$$\begin{aligned}\tau_d &= \left(R_{d,N_f} || R_{q,N_f}\right)\left(C_{d,N_f} || C_{q,N_f}\right) \\ &= \frac{R_d R_q}{R_d + R_q}\left(C_d + C_q\right),\end{aligned} \tag{16}$$

which, typically being $R_d \ll R_q$, can be approximated by

$$\tau_d \approx R_d\left(C_d + C_q\right). \tag{17}$$

Since the photodiode avalanche current is merely related to the charge delivered by the firing microcells, the above $i_{R_d}(t)$ expression, owing to the superposition principle, is then helpfully exploited to model the general case in which more than one pixel is interested by an avalanche event.

Integrating the photodiode current in (14) over time, yields the overall charge delivered by the fired microcells

$$Q = \int_0^{+\infty} i_{R_d}(t)\, dt = I_0 \tau_d, \tag{18}$$

from which, considering the charge due to a single fired pixel (assuming $N_f = 1$), yields the commonly adopted expression for the SiPM gain G as a function of the applied overvoltage V_{OV} and total microcell capacitance $C_d + C_q$

$$G = \frac{Q|_{N_f=1}}{e} = \frac{V_{OV}\left(C_d + C_q\right)}{e}. \tag{19}$$

The gain factor G is a measure of the number of unit electron charges generated in response to a single-pixel ignition, and represents the multiplication factor of a single avalanche.

It should be noted that previously reported SiPM electrical circuits adopting the input current generator as a Dirac's delta pulse to simulate the trigger avalanche discharge might be inherently limited for an accurate modeling of all characteristic features of the output pulse in response to a detected event.

Explicating the SiPM output current in (2), yields

$$I_{R_L}(s) = H(s)\, I_{R_d}(s), \tag{20}$$

where the Laplace transform of the photodiode current is

$$I_{R_d}(s) = L\left\{i_{R_d}(t)\right\} = I_0 \frac{\tau_d}{1 + s\tau_d}. \tag{21}$$

Substituting expressions (11) and (21) into (20), gives

$$I_{R_L}(s) = I_0 \tau_d \frac{1 + s\tau_z}{(1 + s\tau_d)\left(1 + s\tau_{p1}\right)\left(1 + s\tau_{p2}\right)}, \tag{22}$$

from which, by easily inverse Laplace transforming, the complete SiPM output current can be derived as a function of time

$$i_{R_L}(t) = I_0 \tau_d \left(A_d e^{-\frac{t}{\tau_d}} + A_{p1} e^{-\frac{t}{\tau_{p1}}} + A_{p2} e^{-\frac{t}{\tau_{p2}}}\right), \tag{23}$$

with the three exponentials coefficients being given by

$$A_d = \frac{\tau_d - \tau_z}{\left(\tau_d - \tau_{p1}\right)\left(\tau_d - \tau_{p2}\right)} \tag{24}$$

$$A_{p1} = \frac{\tau_{p1} - \tau_z}{\left(\tau_{p1} - \tau_d\right)\left(\tau_{p1} - \tau_{p2}\right)} \tag{25}$$

$$A_{p2} = \frac{\tau_{p2} - \tau_z}{\left(\tau_{p2} - \tau_d\right)\left(\tau_{p2} - \tau_{p1}\right)}. \tag{26}$$

Since $\tau_d < \tau_{p2} < \tau_z < \tau_{p1}$ for feasible values of the circuit model parameters, it follows $A_d < 0$ and $A_{p1}, A_{p2} > 0$.

The complete SiPM time domain response is hence a triple-exponential function consisting of three succeeding intervals, rising, quenching and recovery, reflecting the physical processes undergone by the generated avalanche discharge across the SiPM output terminals. Each of the aforementioned phase is associated with a relevant circuit time constant.

The rising phase (τ_d) corresponds to the time required by an avalanche discharge to be transferred to the read-out load; the quenching phase (τ_{p2}) accounts for the voltage drop across the quenching resistance; the recovery phase (τ_{p1}) originates from the slow recharging of the equivalent diode capacitances.

The amount of charge injected by the firing pixels, represented by the integral of the photodiode current in (18), is delivered as a current signal through the read-out resistor for the entire output pulse duration. In other words, the surface area underneath the output current curve must be equivalent to that lying beneath the photodiode current. Indeed, integrating (23) with respect to time, leads to the same expression as in (18).

To perform a first-order analytical assessment of time constants τ_{p1} and τ_{p2} and provide a graphical comparison with the related curve plots, comparing the denominators in (8) and (11) yields $a_1 = \tau_{p1} + \tau_{p2}$ and $a_2 = \tau_{p1}\tau_{p2}$, from which, assuming $\tau_{p1} \gg \tau_{p2}$, leads to $\tau_{p1} \approx a_1$ and $\tau_{p2} \approx a_2/a_1$. Moreover, neglecting the small contribution of C_m, τ_{p1} and τ_{p2} further simplify into

$$\tau_{p1} \approx R_q\left(C_d + C_q\right) + N R_L C_d \tag{27}$$

$$\tau_{p2} \approx \frac{N R_L R_q C_d C_q}{R_q\left(C_d + C_q\right) + N R_L C_d}. \tag{28}$$

Time constant τ_{p1} is considered as one of the most significant parameters of the SiPM response, since it defines the recovery time of the diode microcells. In fact, the diode voltage takes nearly $5\tau_{p1}$ to recover the original bias conditions within 1% of the final value, and any incoming photon arriving prior to this time, has a lower avalanche triggering probability.

Fig. 3 and Fig. 4 depict the analytical behavior of the complete and approximated expressions of τ_{p1} and τ_{p2}, respectively in (12)–(13) and in (27)–(28), as a function of the total number of cells, N, and for feasible values of the passive elements.

By direct inspection of the above plots, it turns out that the quenching time constant presents a roughly hyperbolic behavior with increasing N, approaching to the constant value of τ_z. On the other side, the recovery time constant almost linearly rises with N from the initial value $R_q(C_d + C_q)$.

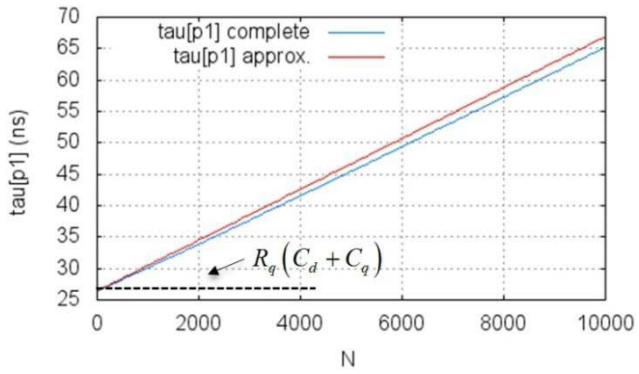

Fig. 3. Recovery time constant of the SiPM output current on a 50-Ω load as a function of N ($R_d = 1\text{k}\Omega$, $R_q = 300\text{k}\Omega$, $C_d = 80\text{fF}$, $C_q = 10\text{fF}$, $C_m = 1\text{fF}$).

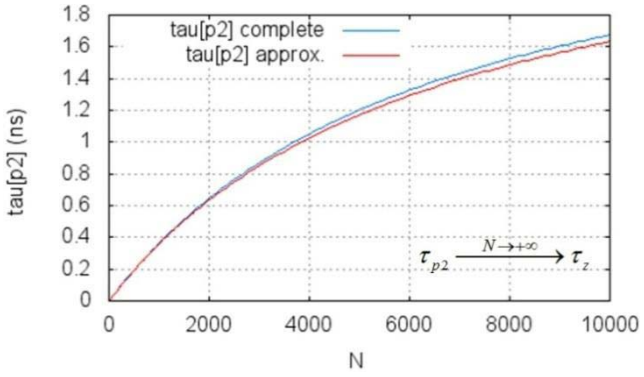

Fig. 4. Quenching time constant of the SiPM output current on a 50-Ω load as a function of N ($R_d = 1\text{k}\Omega$, $R_q = 300\text{k}\Omega$, $C_d = 80\text{fF}$, $C_q = 10\text{fF}$, $C_m = 1\text{fF}$).

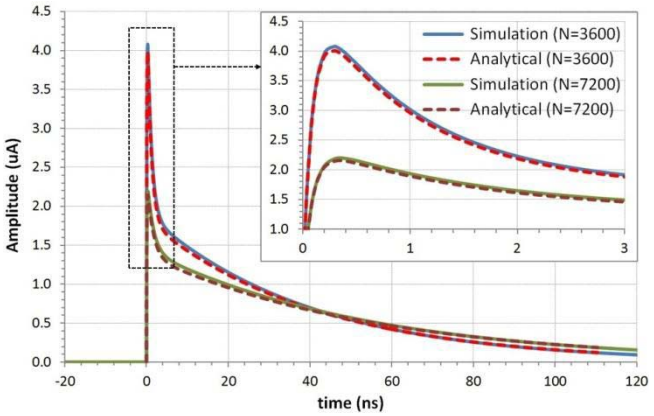

Fig. 5. Analytical and simulated SiPM single-photoelectron output current waveforms, for $V_{OV} = 0.8\text{V}$ and two different values of N ($R_d = 1\text{k}\Omega$, $R_q = 300\text{k}\Omega$, $C_d = 80\text{fF}$, $C_q = 10\text{fF}$, $C_m = 1\text{fF}$).

By nullifying the first derivative in (23) and also assuming $\tau_d \ll \tau_{p1}$, τ_{p2}, τ_z, a first-order approximation of the peak current value can be achieved, yielding

$$I_{peak} \approx I_0 \tau_d \left(A_{p1} + A_{p2}\right) = I_0 \frac{\tau_z \tau_d}{\tau_{p1} \tau_{p2}} \approx \frac{N_f}{N} \frac{V_{OV}}{R_L} \frac{C_q}{C_d \parallel C_q + C_m}, \quad (29)$$

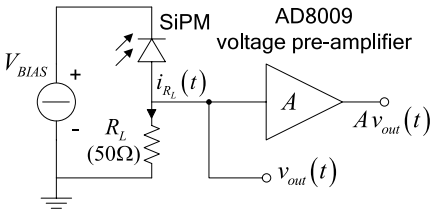

Fig. 6. Schematic overview of the SiPM read-out circuit.

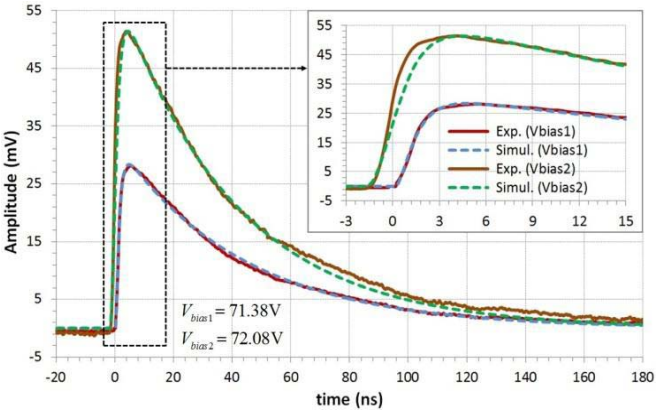

Fig. 7. Simulated and experimental (averaged) output single-photoelectron responses on a 50-Ω load resistor, for $N = 3600$ and two different V_{OV} values.

where $C_d \| C_q$ is the equivalent capacitance $C_d\, C_q / (C_d + C_q)$, resulting from the series connection of C_d and C_q.

IV. Model Validation

To verify the accuracy of the achieved expressions, SPICE simulations are performed for the proposed SiPM equivalent model, and laboratory measurements are also carried out on a physical device.

Analytical and simulated output current pulses under the same circuit parameters are compared in Fig. 5 for two values of N. As expected, with increasing values of N, the simulated single output current pulse decreases its peak current and enlarges the associated time constants while keeping the same time integral, in good agreement with the analytical expressions obtained in (23).

Analytical and measured output pulse waveforms are compared together for a $3\times3\text{mm}^2$ 50-μm pitch Hamamatsu device. Tests are carried out at the Catania astrophysical Observatory Laboratory for Detectors (COLD) on the assembled read-out circuit schematically sketched in Fig. 6. Pulse waveforms are acquired on a Lecroy digital oscilloscope featuring a 4-GHz bandwidth, a 20-GS/s sampling rate, and an intrinsic 0.5-mV baseline noise. SiPM single photoelectron responses are captured with the detector kept in dark.

Circuit model parameters of the Hamamatsu device are estimated based on experimental measurements and the extracted values are summarized in Table I. Parameters extraction is accomplished through a dedicated characterization procedure [10], [11]. In particular, the photodiode resistances are obtained from the slope of the forward I-V static

TABLE I
ESTIMATED MICROCELL MODEL PARAMETER VALUES

SiPM S/N	Hamamatsu S11828-3344MX				
Parameter	R_d (Ω)	R_q (Ω)	C_d (F)	C_q (F)	C_m (F)
Values	1k	290k	78f	8f	1f

characteristics; the charge delivered after a Geiger discharge is derived by applying a linear fit to the peak positions in a signal charge histogram; and the total microcell capacitance and breakdown voltage are respectively determined from the slope and x-axis intercept of the associated curve relating the measured charge to the external operating voltage. Measures are performed at 25°C, at which a breakdown voltage of 70.5V is obtained.

The adopted electrical circuit of the SiPM detector is simulated, with the SPICE model of the voltage pre-amplifier included in the simulation scheme cascaded to the output load, to account for the frequency shaping in the rising edge of the measured signal (due to the limited amplifier bandwidth) and attain an accurate waveform comparison.

For a single firing cell, data outputs of both simulated and measured output voltage pulses are merged together in Fig. 7 for N =3600, for two different overvoltage values (0.88V and 1.58V) and a 36-dB pre-amplifier gain factor. As inspected, the simulated and experimental waveforms are well-matched, validating the above analysis.

V. CONCLUSION

A systematic theoretical analysis of an accurate SiPM electrical model is carefully addressed to reproduce and predict the SiPM output response. The adopted model allows for an accurate analytical analysis of the detector behavior. Analytical, simulation and experimental comparisons of the pulse responses are performed to demonstrate the predictive capabilities of the adopted analysis. Measurements results are in good agreement with expectations and validate the accuracy of the achieved analytical expressions.

REFERENCES

[1] G. Condorelli *et al.*, "Extensive electrical model of large area silicon photomultipliers," *Nucl. Instrum. Methods Phys. Res. A, Accel. Spectrometers Detectors Assoc. Equip.*, vol. 654, no. 1, pp. 127–134, 2011.
[2] S. Cova, M. Ghioni, A. Lacaita, C. Samori, and F. Zappa, "Avalanche photodiodes and quenching circuits for single-photon detection," *Appl. Opt.*, vol. 35, no. 12, pp. 1959–1976, 1996.
[3] N. Pavlov, G. Mæhlum, and D. Meier, "Gamma spectroscopy using a silicon photomultiplier and a scintillator," in *Proc. IEEE Nucl. Sci. Symp. Conf. Rec.*, Oct. 2005, pp. 173–180.
[4] S. Seifert *et al.*, "Simulation of silicon photomultiplier signals," *IEEE Trans. Nucl. Sci.*, vol. 56, no. 6, pp. 3726–3733, Dec. 2009.
[5] F. Corsi *et al.*, "Electrical characterization of silicon photomultiplier detectors for optimal front-end design," in *Proc. IEEE Nucl. Sci. Symp. Conf. Rec.*, Nov. 2006, pp. 1276–1280.
[6] A. K. Jha, H. T. van Damm, M. A. Kupinski, and E. Clarkson, "Simulating silicon photomultiplier response to scintillation light," *IEEE Trans. Nucl. Sci.*, vol. 60, no. 1, pp. 336–351, Feb. 2013.
[7] D. Marano *et al.*, "Improved SPICE electrical model of silicon photomul-tipliers," *Nucl. Instrum. Methods Phys. Res. A*, vol. 726, pp. 1–7, Aug. 2013.
[8] D. Marano *et al.*, "Silicon photomultipliers electrical model extensive analytical analysis," *IEEE Trans. Nucl. Sci.*, vol. 61, no. 1, pp. 23–34, Nov. 2013.
[9] G. Giustolisi, G. Palumbo, P. Finocchiaro, and A. Pappalardo, "A simple extraction procedure for determining the electrical parameters in silicon photomultipliers," in *Proc. IEEE ECCTD*, Sep. 2013, pp. 1–4.
[10] G. Bonanno *et al.*, "Characterization measurements methodology and instrumental set-up optimization for new SiPM detectors—Part I: Electrical tests," *IEEE Sensors J.*, to be published.
[11] G. Bonanno *et al.*, "Characterization measurements methodology and instrumental set-up optimization for new SiPM detectors—Part II: Optical tests," *IEEE Sensors J.*, to be published.

Davide Marano was born in Catania, Italy, in 1979. He received the M.Sc. (*summa cum laude*) degree in electronic engineering from the University of Catania, and the Ph.D. degree from the Dipartimento di Ingegneria Elettrica, Elettronica e dei Sistemi, University of Catania, in 2006 and 2010, respectively. Since 2012, he has been with Osservatorio Astrofisico di Catania, Istituto Nazionale di Astrofisica, as a Junior Design Engineer. His original research projects have been focused on analog integrated circuits, with particular emphasis devoted to feedback amplifiers and frequency compensation. Subsequently, his interests have also embraced digital integrated circuits. His main research activities include the design of CMOS high-performance integrated circuits, low-power amplifiers, and high-speed buffers for liquid crystal display drivers. He has co-authored many scientific papers on mixed electronics.

Massimiliano Belluso was born in Catania, Italy, in 1967. He received the Diploma degree in electronics from the Archimede Institute of Catania in 1985. In 1987, he joined STMicroelectronics, Catania, as a Junior Designer. From 1992 to 2000, he served as a High-School Instructor of Electronics. Since 2003, he has been with Osservatorio Astrofisico di Catania, Istituto Nazionale di Astrofisica, as a Senior Designer of Electronic Systems. His primary research interests include solid-state detectors for astrophysical applications, intensified charge-coupled devices (CCDs), imaging detectors, active pixel sensors, and photon-counting systems. He is mainly involved in the electronic design of CCD controllers and custom electronics using field programmable gate array. He has co-authored several technical and scientific articles. He holds an international and an Italian patent on photon-counting systems.

Giovanni Bonanno was born in Catania, Italy, in 1955. He received the M.Sc. degree in physics from the University of Catania in 1980. Since 2001, he has been serving as a Full Astronomer of Astrophysical Technologies with Osservatorio Astrofisico di Catania, Istituto Nazionale di Astrofisica. His main research interests and activities include silicon photomultiplier detectors, charge-coupled devices, and photon-counting systems for ground and space astrophysical applications. He is mainly involved in full electronic testing, measurements and characterizations of imaging detectors, and related electronic instrumentation. He has co-authored several technical and scientific papers about detectors and electronic controllers. He holds one national patent on a photon-counting system. He has been responsible for the design and realization of electronic control systems for the instrumentation of the Italian telescope Galileo (TNG) in Las Palmas, the stellar site G. Fracastoro on Mount Etna, and some space projects.

Sergio Billotta was born in Catania, Italy, in 1976. He received the M.Sc. degree in physics from the University of Catania in 2003. In 2003, he joined the STMicroelectronics, Catania, as a Research Consultant. Since 2004, he has been with Osservatorio Astrofisico di Catania, Istituto Nazionale di Astrofisica, Catania, as a Full Researcher. His main research interests and activities include single-photon avalanche photodiodes, silicon photomultiplier detectors, charge-coupled devices, active pixel sensors, imaging detectors, and photon-counting systems for ground and space astrophysical applications. He is mainly involved in full electronic testing, measurements, and characterizations of imaging detectors. He has co-authored many technical and scientific papers, and is currently joining interferometer and quantum astronomy programs.

Alessandro Grillo was born in Francavilla di Sicilia, Italy, in 1968. He received the M.Sc. degree in computer science from the University of Catania in 2005. From 2006 to 2007, he was a Collaborator with the project TriGrid Virtual Laboratory at Osservatorio Astrofisico di Catania (OACT), Istituto Nazionale di Astrofisica, as a System Manager for HPC-grid systems developing network environments for the theoretical virtual observatory implementation. From 2007 to 2011, he collaborated with Consorzio COMETA as a Technologist System Manager for the administration of grid computing and storage systems and the optimization of high-performance computing environments on parallel systems based on Linux cluster. Since 2011, he has been involved in developing software for the control interfaces of laboratory equipment in Java, C, and C++ languages. He has participated in the development of web science portals and has co-authored several scientific publications with the activities at OACT. He often participates in conferences and meetings on specialized topics about computing and ICT.

Salvatore Garozzo was born in Catania, Italy, in 1978. He received the M.Sc. degree in electronic engineering from the University of Catania in 2004, upon discussing a dissertation on AMOLED display drivers, performed at STMicroelectronics, Catania. In 2010, he was a Construction Supervisor with a company of electrical systems. Since 2006, he has been serving as a Professor of Electronics at the Secondary High School. Since 2012, he has been with Osservatorio Astrofisico di Catania, Istituto Nazionale di Astrofisica, as a Junior Design Engineer. His main research activities include the analysis and design of analog and mixed-signal integrated circuits. He is involved in the electronic design of high-performance integrated circuits and custom electronics based on field programmable gate array.

Giuseppe Romeo was born in Catania, Italy, in 1976. He received the M.Sc. degree in electronic engineering from the University of Catania in 2008, upon discussing a dissertation about output resistance adaptation in CMOS buffer amplifiers and buffers. In 2008, he received the certification of skills in electronic design of integrated circuits from the Dipartimento di Ingegneria Elettrica, Elettronica e dei Sistemi, University of Catania. In 2008, he was a Marketing Category Management Supervisor at Euronics Italy. Since 2009, he has been a Teacher of Electronics and Mathematics in secondary schools. Since 2012, he has been a member of Osservatorio Astrofisico di Catania, Istituto Nazionale di Astrofisica, as a Junior Design Engineer with the Laboratory Characterization of Detectors.